Localization of CO_2 leakage from transportation pipelines through low frequency acoustic emission detection

Xiwang Cui[a], Yong Yan[b,a], Yifan Ma[a] , Lin Ma[c,a], Xiaojuan Han[a]

[a]*School of Control and Computer Engineering, North China Electric Power University, Beijing 102206, P R China*

[b]*School of Engineering and Digital Arts, University of Kent, Canterbury, Kent, CT2 7NT, UK*

[c]*Department of Mechanical Engineering, University of Sheffield, Sheffield, S10 2TN, UK*

Abstract:

Carbon Capture and Storage is a technology to reduce greenhouse gas emissions. CO_2 leak from high pressure CO_2 transportation pipelines can pose a significant threat to the safety and health of the people living in the vicinity of the pipelines. This paper presents a technique for the efficient localization of CO_2 leakage in the transportation pipelines using acoustic emission method with low frequency and narrow band sensors. Experimental tests were carried out on a lab scale test rig releasing CO_2 from a stainless steel pipe. Further, the characteristics of the acoustic emission signals are analyzed in both the time and the frequency domains. The impact of using the transverse wave speed and the longitudinal wave speed on the accuracy of the leak localization is investigated. Since the acoustic signals are expected to be attenuated and dispersed when propagating along the pipe, empirical mode decomposition, signal reconstruction and a data fusion method are employed in order to extract high quality data for accurate localization of the leak source. It is demonstrated that a localization error of approximately 5% is achievable with the proposed detecting system.

Keywords: CO_2; Leak localization; Acoustic emission; Empirical mode decomposition.

1. Introduction

Carbon Capture and Storage (CCS) is a major emerging technology to reduce CO_2 emissions from power generation and other industrial processes. It enables a sustainable use of fossil fuels for power generation with a substantially reduced level of emissions of CO_2 into the atmosphere [1]. Transportation of CO_2 through over long distances pipelines is an essential part of the CCS technology to deliver the captured CO_2 to its permanent storage sites, such as depleted oil and gas reservoirs and/or deep saline

formations. However, any accidental leak from a CO_2 pipeline can cause direct economic loss and environmental damage. When the pipeline is within a densely populated area, CO_2 leak can pose a significant threat to the safety and health of local residents as CO_2 will become toxic at high concentrations [2]. Therefore, it is imperative to detect, locate and stop any accidental leak of CO_2 quickly when it occurs.

A number of methods have been proposed in the past to detect toxic gas leak, ranging from traditional manual inspection by survey crews to more advanced satellite spectral imaging [3-5]. Sensors for CO_2 leak detection based on physical [6], chemical [7] and biological principles [8] have been proposed and developed, such as those based on tracer gas, electromagnetic scanning, optical fiber sensing, infrared thermography and flow equilibrium [9]. Recently, a miniaturized CO_2 sensor based on the principle of infrared absorption has been developed by Zhang et al. [10]. The sensor consists of an infrared source, an air chamber, an infrared receiver, and two sapphire windows. Kasyuticha and Martin [11] developed a CO_2 sensing instrument based on direct absorption spectroscopy. The instrument consists of a continuous-wave thermoelectrically cooled (TEC) distributed quantum cascade laser and an optical cell. Technologies based on vegetation response to leaked CO_2 have also been developed for CO_2 leak detection using spectral vegetation indices [12] as CO_2 can deplete oxygen in the soil.

The majority of these detection systems are, however, complex, cumbersome in arrangement and expensive to set up and operate. In addition, studies conducted with these technologies are usually used to detect leak in a specific place or a small scale region, therefore a large number of sensors are thus required to cover a long pipeline. Very limited research has been undertaken for the efficient detection and localization of CO_2 leak from transportation pipelines.

Leak detection using acoustic emission (AE) sensors is a technology that can sense and locate leaks from pinhole size perforations, cracks and ruptures in pipelines. It has been proposed and researched in leak detection of natural gas and oil pipelines [13], and in principle this technology may also be suitable for CO_2 leak localization. In comparison with other techniques, the AE method has advantages of non-intrusiveness, low cost, simple structure, high sensitivity and easy installation and thus has a good potential for CO_2 leak detection and localization.

When the CO_2 leak occurs from a pressurized pipeline, a strong turbulent jet flow may be produced together with a strong acoustic emission due to a sudden pressure drop

from the pipeline pressure to the environment. AE devices can be used to detect and locate the source of the leak based on the analysis of the acoustic signals received. A reference standard has been proposed for establishing and evaluating AE equipment for pipeline leak detection [14]. This reference standard has been proved to be valuable not only for evaluating the AE equipment, but also for characterizing the source mechanisms as part of an integrated approach to assess AE leak detection and localization technology.

The acoustic energy of a gas jet usually has a wide spectral range from 1 kHz to 1 MHz, although the majority of energy is confined to the moderately high frequency band of 175 kHz – 750 kHz [15]. Mostafapour and Davoudi researched the vibration behavior of a gas pipeline (5 bar air) using AE sensors with an operating frequency range from 50 kHz to 500 kHz. They have found that the AE signals captured are in the range between 150 kHz and 300 kHz [16]. Therefore, most research on this topic focuses primarily on high frequency (>100 kHz) AE sensors. High frequency AE sensors have an advantage of having a high performance against ambient noise. However, since the pipelines used to transport CO_2 are typically long distance and can attenuate a substantial proportion of the high-frequency AE signals, it is believed that the performance of low-frequency AE sensors for the leak detection from CO_2 pipelines is worth investigating.

This paper presents the principle and application of AE sensors in the low frequency and narrow band for long distance leak localization on a CO_2 pipeline. Since the AE signals are expected to be attenuated and dispersed along the pipeline walls, which makes the signals difficult to analyze, empirical mode decomposition (EMD), signal reconstruction and a data fusion method are deployed in order to accurately locate the leak source.

2. Methodology

2.1. Acoustic emission from a gas leak

Acoustic emission from a leaking pipe is usually caused by the high pressure turbulent jet flow that is produced through a hole or crack on the pipeline. The AE signal normally has a wide frequency band but has a close correlation with the flow conditions and the characteristics of the pipeline. It contains unique features of the source of the leak, such as the size of the hole and the distance that the signal has traveled through from its source, and therefore using a correct signal processing

algorithm the leak can be detected and located accurately.

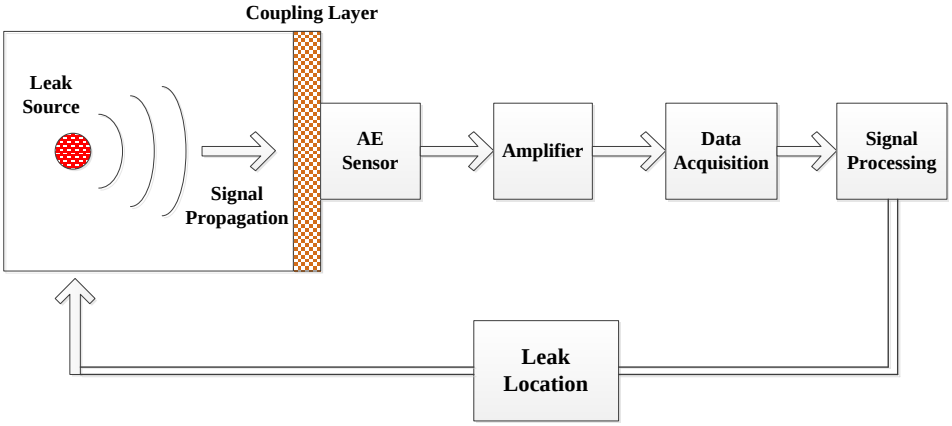

Fig.1. Principle of the leak localization system based on AE method.

Fig. 1 shows the principle of the leak localization system based on the AE method. When a leak occurs on a pressurized CO_2 pipeline, the AE signal generated propagates along the pipeline and can be picked up by AE sensors installed on the pipeline wall. The signals received are amplified and processed to locate the source of the leak.

The AE sensor is a key component of the leak localization system. The sensor selection should be based on the frequency range of the signal of the leak and its characteristics of propagation. High frequency sensors have a clear advantage of immunity from the ambient noise which usually distributes in the low frequency range. Common ambient noise comes from pedestrians and motor vehicles around the pipelines and from the operation of various valves in the pipeline. However, as the pipelines used to transport CO_2 are very long, high frequency AE signals can be seriously attenuated during propagation and thus become very difficult to pick up over a long distance. Earlier research compared the attenuations of high and low frequency signals along a steel pipeline of 159mm external diameter and 4mm wall thickness [17], as shown in Fig. 2. The AE source was simulated by Nielsen-Hsu Pencil Lead Break Test [18]. The signals produced were detected by using high and low frequency sensors with resonant frequencies of 30 kHz and150 kHz, respectively.

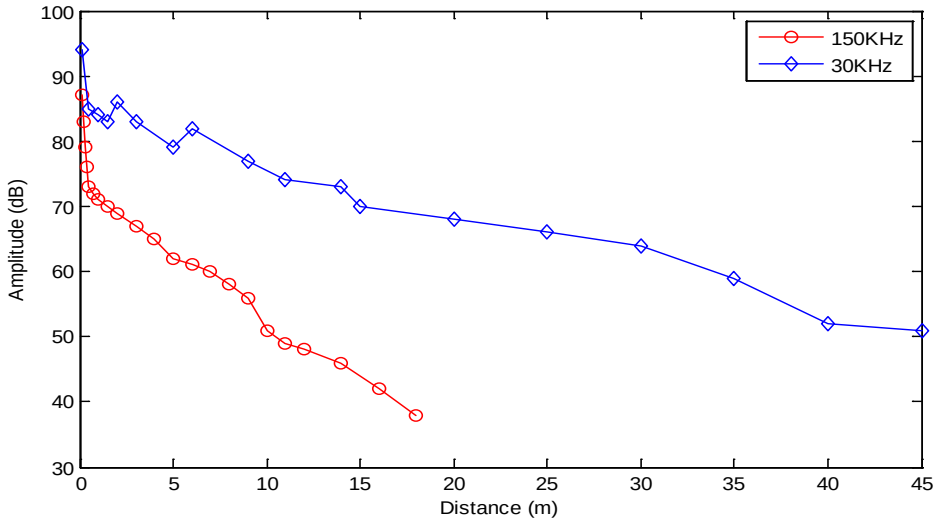

Fig. 2. AE signal attenuation on a pipeline [17].

The strength of the signal received by the high frequency sensor (150 kHz) has dropped by over 50% in less than 20 meters and it cannot be detected anymore using this sensor after 20 meters away from the source. On the contrary, the strength of the signal received by the low frequency sensor (30 kHz) decreases moderately and can still be picked up by the sensor with a relatively high intensity even over 45 meters away, showing a significant potential of low frequency sensors for long-distance pipeline leak detection.

In addition to the signal attenuation, the AE signal will be dispersed when propagates along the pipeline wall. Dispersion makes the AE signal produce a greater distortion and cause additional difficulty in locating the source of the leak. Fig. 3 shows an AE signal dispersion in a 1mm thick aluminum plate as reported by Wilcox, et al. [19]. It can be seen that the original signal waveform has been seriously distorted with the increase in both the distance and the time of the propagation. The dispersion increases the duration and decreases the amplitude of the wave packet and this makes the recognition and extraction of the characteristics of the signals more difficult after they have travelled over a long distance. Therefore, mode decomposition and signal reconstruction should be considered in order to locate the leak accurately.

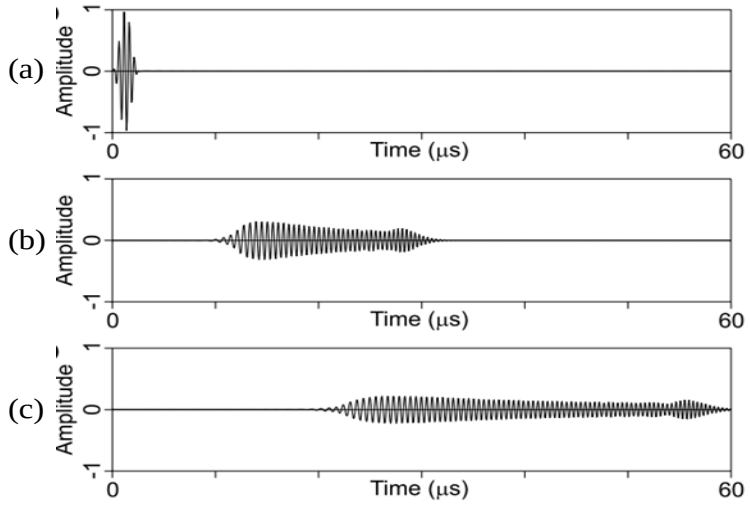

Fig. 3. Schematic diagram of AE signal dispersion: (a) close to the source, (b) 50 mm from the source and (c) 100 mm from the source [19].

2.2. Empirical mode decomposition

The attenuation and dispersion of the AE signals usually result in a small correlation coefficient leading to a large localization error. Therefore, it is not accurate or sometimes even not feasible to locate the leak source by cross correlating the AE signals directly. In order to solve this problem, appropriate mode decomposition algorithm is necessary. Empirical mode decomposition (EMD) is one of the effective approaches to processing non-linear and non-stationary signals. It is an adaptive signal processing method which does not need priori information about the signal to be processed. The leak AE signals have obvious non-linear and non-stationary characteristics and can be decomposed in both time and frequency domains using EMD.

EMD is usually realized by taking the signal as being composed of a series of oscillating components, referred to as IMFs (intrinsic mode functions). A function is called an IMF when it satisfies the following two conditions [20]:

Condition (i) The number of IMF extrema (the sum of the maxima and minima) and the number of zero-crossings must either be equal or differ at most by one;

Condition (ii) At any point of an IMF, the mean value of its upper envelope and lower envelope shall be zero.

Condition (i) is to assure that the signal has a narrow band characteristic, and Condition (ii) is to assure that the instantaneous frequency will not have the unwanted fluctuations induced by an asymmetric wave.

The computational process of the EMD is as follows [21, 22]:

(i) For a signal X(t), let $m_1(t)$ be the mean value of its upper and lower envelopes as determined from a cubic-spline interpolation of local maxima and minima.

(ii) Compute $h_1(t)$ as follows:

$$h_1(t) = X(t) - m_1(t) \tag{1}$$

(iii) If $h_1(t)$ satisfies the definition of an IMF given above, $h_1(t)$ will be the first oscillating component, IMF1. If not, then $h_1(t)$ will be treated as a new signal X(t) and repeat the steps (i) and (ii) until $h_1(t)$ satisfies the definition of an IMF.

(iv) Calculate the residual r by subtracting the first IMF component $h_1(t)$ from $X(t)$:

$$r_1(t) = X(t) - h_1(t) \tag{2}$$

(v) Let $r_1(t)$ be the new signal $X(t)$, repeat the steps (i) - (iv), and then separate the new IMF components as follows:

$$\begin{aligned} r_2(t) &= r_1(t) - h_2(t) \\ &\cdots \\ r_n(t) &= r_{n-1}(t) - h_n(t) \end{aligned} \tag{3}$$

The above decomposition process will be terminated if the final residual of the signal, $r_n(t)$ or $h_n(t)$, is less than a prescribed value or $r_n(t)$ become a monotonic function. Then the original signal $X(t)$ can be represented by the sum of all the IMF components and the final residue $r_n(t)$ as follows:

$$X(t) = \sum_{i=1}^{n} h_i(t) + r_n(t) \tag{4}$$

In this paper, EMD is employed to decompose the leak AE signal in order to remove the noise and extract the signal features. A reconstructed signal based on the signal features is used to locate the leak source.

2.3. Leak localization

Leak localization based on the AE method usually uses a pair of AE sensors. Fig. 4 shows the common arrangement of the two sensors, i.e. one on each side of the leak hole.

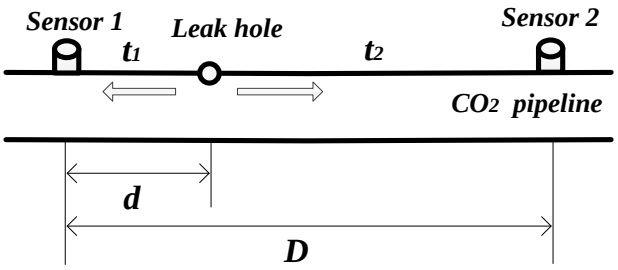

Fig. 4. Schematic diagram of the sensing arrangement.

In a gas releasing test, the location of the source can be determined by calculating the time difference between the two AE signals. If the speed of the AE wave traveling along the pipe wall is known, then the distance, *d*, of the source from Sensor 1 is calculated from:

$$d = \frac{D - v\Delta t}{2} \tag{5}$$

where D is the distance between the two sensors, v is the speed of AE wave travelling along the pipeline, and Δt is the time difference of the two AE signals. Clearly, the two key tasks of this localization method in the experiments are to measure the speed v and the time difference Δt.

Typically a gas leak produces two types of AE wave, i.e. transverse wave and longitudinal wave, both of which propagates along the pipeline and can be detected by the AE sensors. The speeds of the AE waves can usually be acquired by querying the technical manual of the pipeline [23]. However, due to the complex design and structure of the pipeline, the speed of AE wave can change along the pipeline even when the same material is used for the entire pipeline [24]. Therefore, the speed measurement should take into consideration the influence of both pipe materials including its inhomogeneity and the structure of the pipeline.

In this paper, the speed of AE wave is measured through the Nielsen-Hsu Pencil Lead Break Test [18], which can produce a pulse signal with a sharp rising front edge and an exponential attenuation decline period afterwards.

The time difference is estimated through cross correlation computation [25]:

$$R_{xy}[m] = \frac{\sum_{k=0}^{N-|m|-1} x_k y_{k+m}}{\sqrt{\sum_{k=0}^{N-1} x_k^{\,2}} \sqrt{\sum_{k=0}^{N-1} y_k^{\,2}}} \tag{6}$$

where x_k and y_k denote the two AE signals received by the two sensors and N is the length of the signal. The time difference corresponds to the location of the dominant peak in the correlation function $R_{xy}[m]$ whilst the peak value is the correlation coefficient representing the similarity of the two signals.

3. Experimental system

In order to analyze the characteristics of the AE signals due to CO_2 leak and to evaluate the AE method for identifying the location of the leak source, experimental work was carried out on a six-meter-long stainless steel pipeline of 50 mm external diameter and 2 mm wall thickness. A continuous release of CO_2 at a pressure of 3bar from a 2 mm diameter hole on the pipeline was created. Four identical AE sensors were mounted sequentially along the pipeline using adhesive tape and vacuum grease couplant. The AE signals were pre-amplified using smart AE amplifiers with a bandwidth of 10 kHz–1 MHz and a gain of 40 dB. A 4-channel holographic AE signal analyzer (DS-8A) was used for waveform acquisition at a sampling rate of 500 kHz. The schematic and the test rig for the CO_2 leak detection system employed are shown in Fig. 5 and Fig. 6.

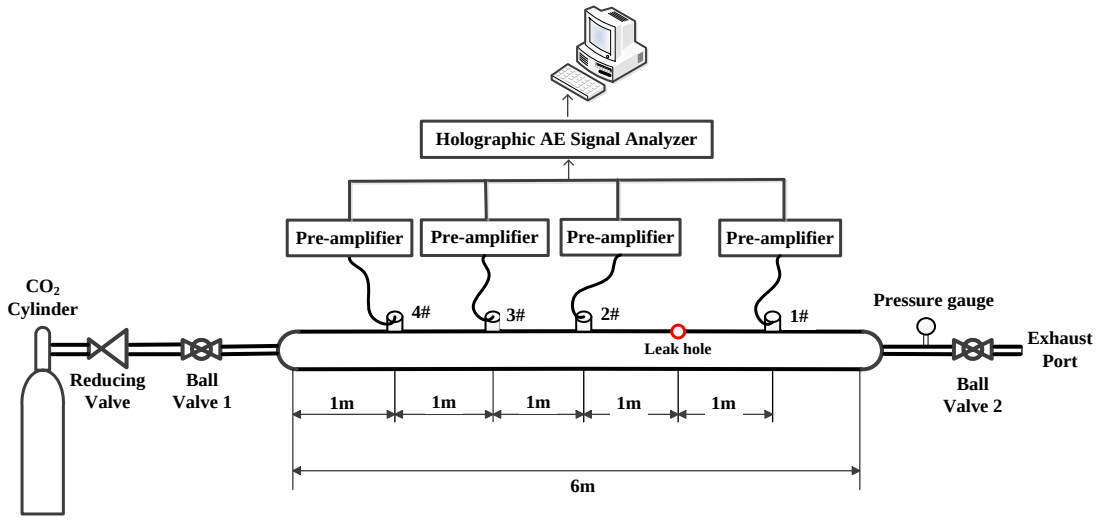

Fig. 5. Schematic of the experimental CO_2 leak detection system.

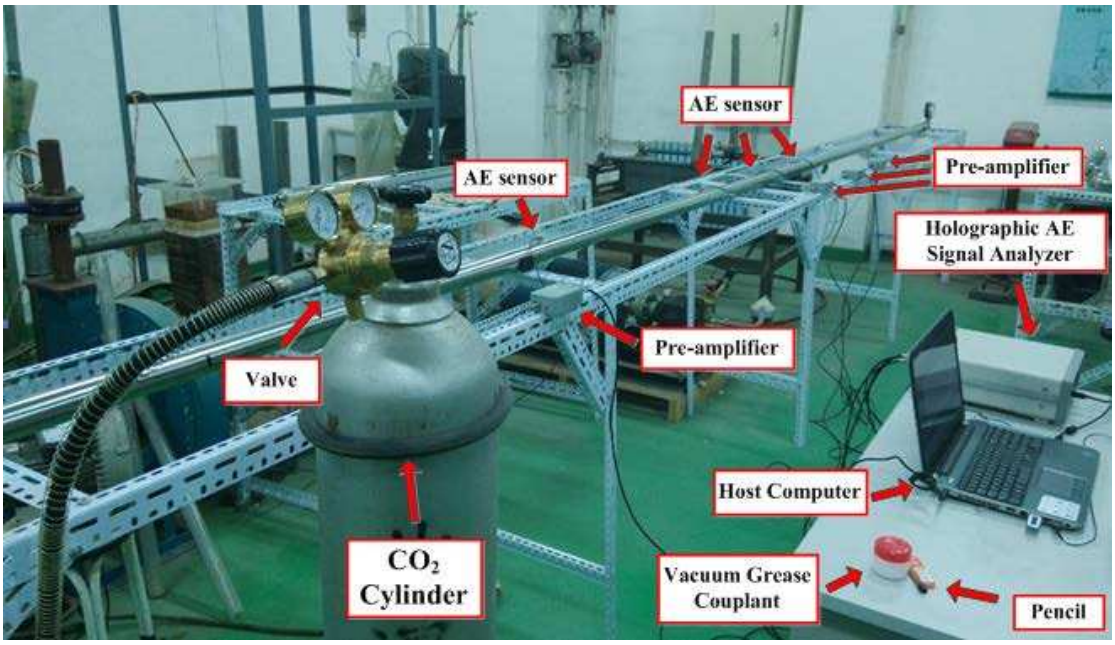

Fig. 6. Test rig for the CO_2 leak detection system

The AE sensors used are SR40M and supplied by Soundwel Technology Co. Ltd with a low frequency and narrow band. The sensor specifications and typical frequency response characteristics are shown in Table 1 and Fig. 7.

Table 1
Sensor specifications

Sensor model	SR40M
Dimension DIA*HT (mm)	22*36.8
Operating Temperature (^oC)	-20-120
Interface Type	M5-KY
Operating Frequency Range (kHz)	15-70
Peak Sensitivity (dB)	>75

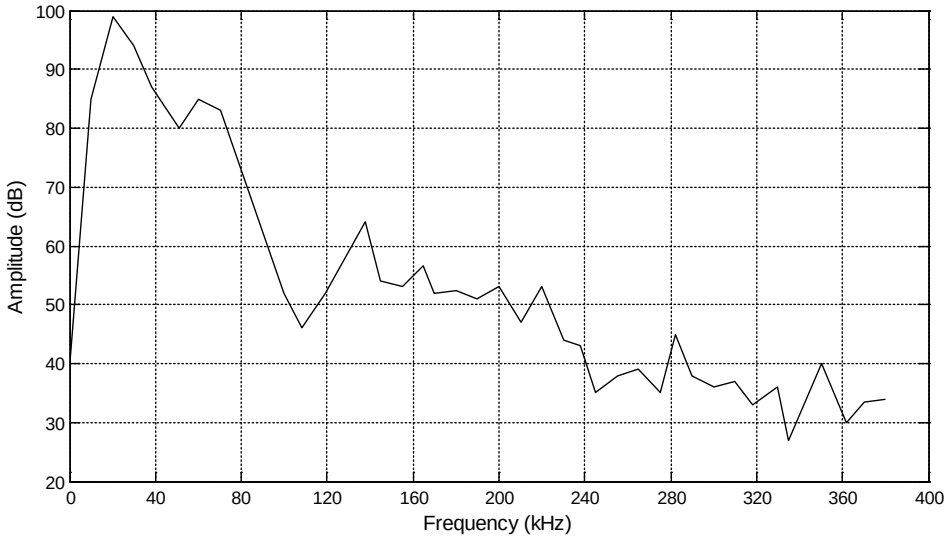

Fig. 7. Frequency response of the SR40M sensor.

Fig. 7 shows this sensor has a good sensitivity (over 80 dB) in the frequency band from 15 kHz to 70 kHz. In this frequency band, the sensor can effectively avoid the influence of the audible sound.

4. Experimental results and discussion

4.1. Measurement of the AE wave speed

In order to measure the speed of the AE wave travelling on the pipe wall, an AE source was simulated by conducting the Nielsen-Hsu Pencil Lead Break Test. The location of the lead break point was between sensor 2 and the leak hole. Sensors 2 and 3 on the same side of the lead break point were selected to receive the AE signal generated, because these two sensors are in the middle part of the pipeline and can effectively avoid the effect of the echo from the end of the pipeline. An HB pencil with a diameter of 0.5 mm was used to generate an AE wave. The pencil lead was placed at an angle of approximate 30 degrees with the pipeline surface and the length of the lead was 2.5 mm. Fig. 8 shows the pencil lead break test and resulting waveforms received by sensors 2 and 3.

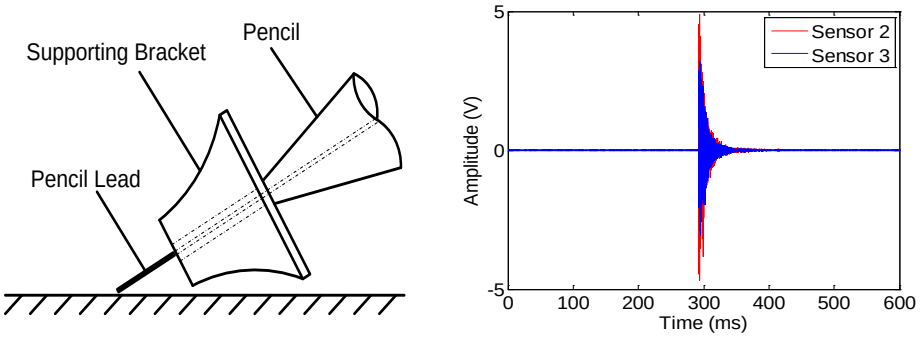

(a) Test arrangement (b) Resulting waveforms

Fig. 8. Pencil lead break test.

As discussed in the previous section, two types of AE waves will propagate along the pipeline, i.e. transverse wave and longitudinal wave. These two types of waves are clearly seen in Fig. 9.

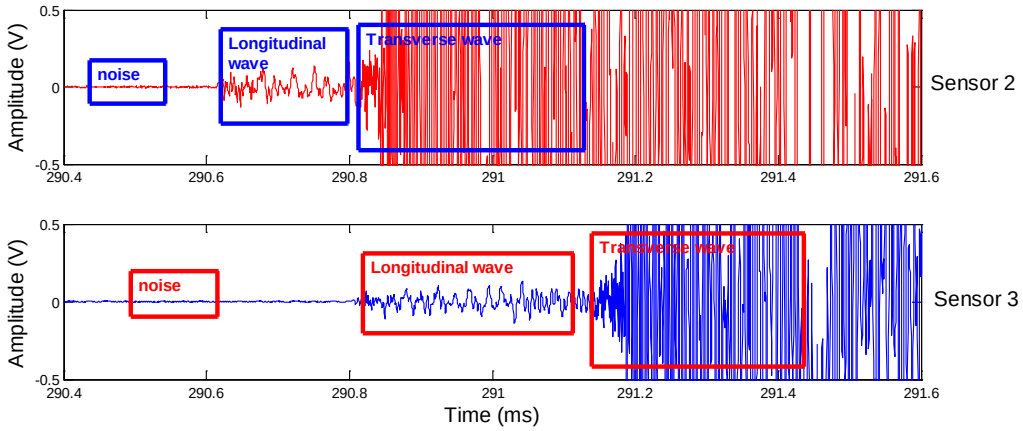

Fig. 9. Zoomed-in waveforms from the pencil lead break test.

The longitudinal wave usually has a higher speed and lower amplitude than the transverse wave. Thus, it can be received earlier by the sensors. The arrival time of the transverse and longitudinal waves can be easily distinguished from the zoomed-in waveforms. Fig. 9 also indicates that the noise of the detection system is very low with a maximal amplitude of no greater than 5 mV.

Since the distance between Sensors 2 and 3 is known (1 m). Therefore the speeds of the transverse wave and the longitudinal wave can be calculated. The lead break tests were repeated 10 times. The average speeds of the longitudinal and transverse waves are found to be 5070 m/s and 3268 m/s, respectively. The impact of using these two

different speeds on the accuracy of the leak localization will be discussed later.

4.2. Characteristics of the leak AE signal

A set of leak experiments was designed and conducted to study the characteristics of the AE signal. During the experiments, the pressure regulating valve maintained the pressure in the pipeline at 3 bar. The AE signals were recorded as shown in Fig. 5. The time domain waveforms and frequency spectra of the AE signals from the four sensors are plotted in Fig. 10 and Fig. 11, respectively.

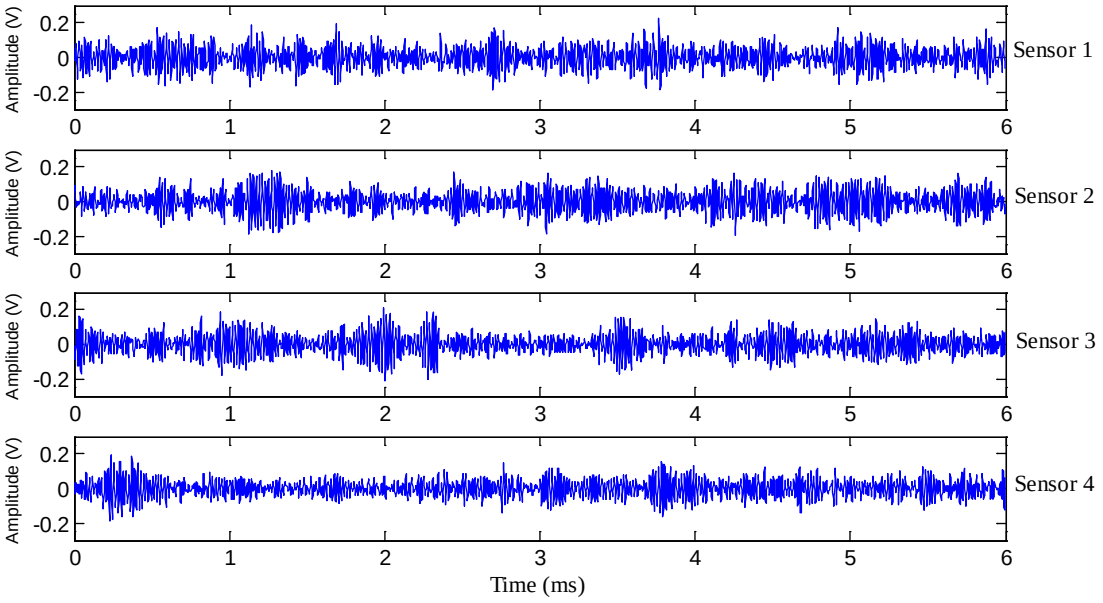

Fig. 10. Time domain signal waveforms.

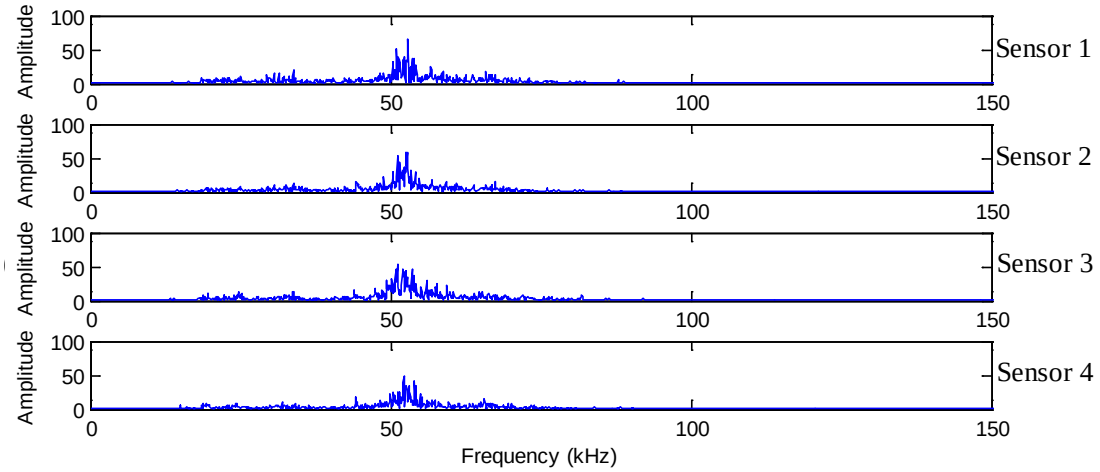

Fig. 11. Frequency spectra of the signals.

From the frequency spectra, it can be seen that the energy of the AE signals concentrates in the band of 40 kHz to 70 kHz. It demonstrates that the AE sensors have a good performance to detect low frequency and narrow band signals.

It can be seen that the signal from sensor 4 has the lowest in amplitude (Fig. 10) because sensor 4 is the farthest from the leak source and hence the strongest attenuation of the signal. The same trend is evident in the frequency domain (Fig. 11). The degree of attenuation of the AE signals can be quantified in terms of signal energy:

$$E = \sum_{n=0}^{N-1} x_n^{\,2} \tag{7}$$

where x_n is the sampled AE signal. The energies of the four AE signals are shown in Fig. 12.

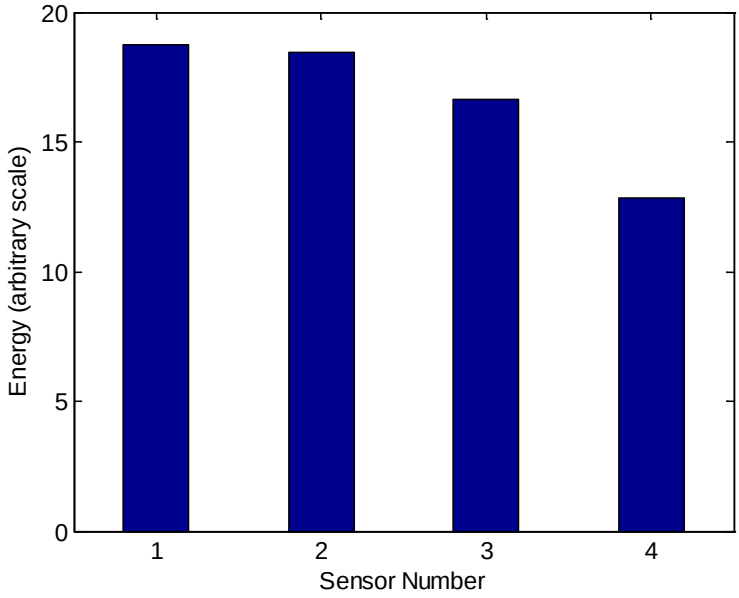

Fig. 12. Energies of the AE signals.

Fig. 12 shows that signals from sensors 1 and 2 have higher energies than those from sensors 3 and 4. Due to the linear installation of the sensors on the pipeline, we can conclude that the leak source should be located between sensors 1 and 2. Localizing the source of the leak requires further analysis using signal decomposition and reconstruction techniques.

4.3. Empirical mode decomposition of the AE signals

The original AE signals are decomposed in both time and frequency domains using the EMD method as discussed in the previous section. The EMD can separate the major

energy components of a signal from the rest of the signal, in particular, those originate for various noises. The major energy components of the signal can be used to estimate the location of the leak source. Fig. 13-16 show the decomposition results of the original signals from the four sensors.

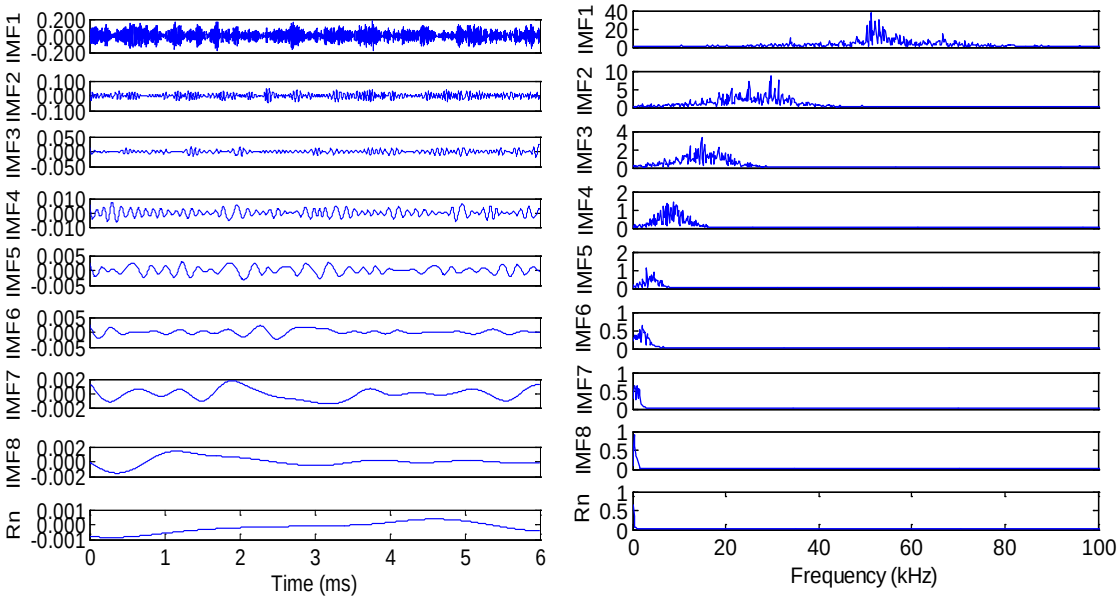

Fig. 13. EMD results of the signal from sensor 1.

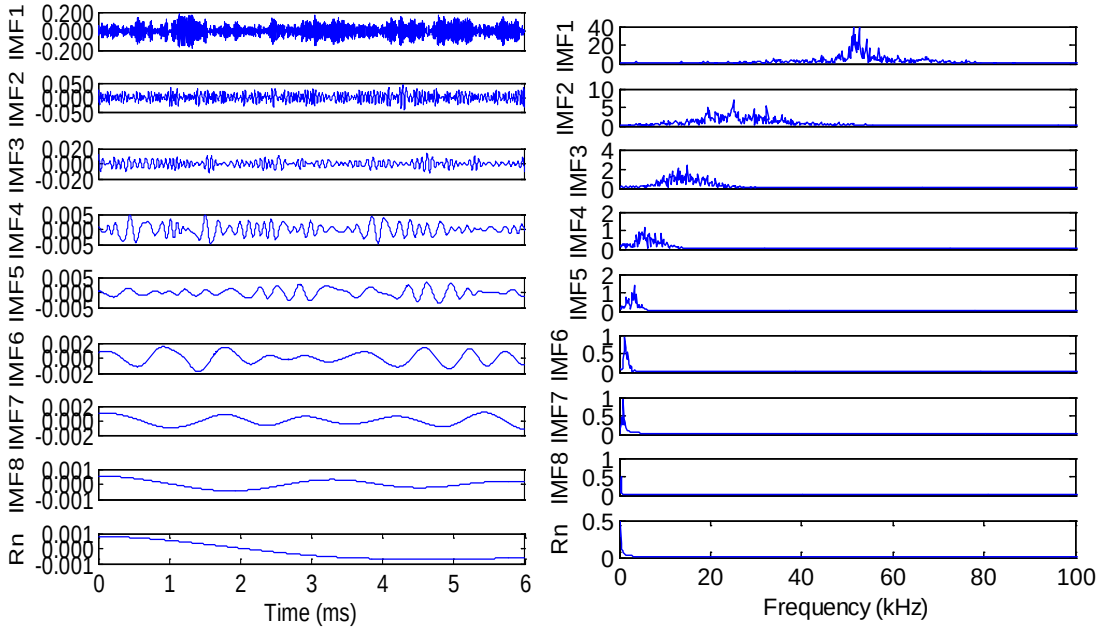

Fig. 14. EMD results of the signal from sensor 2.

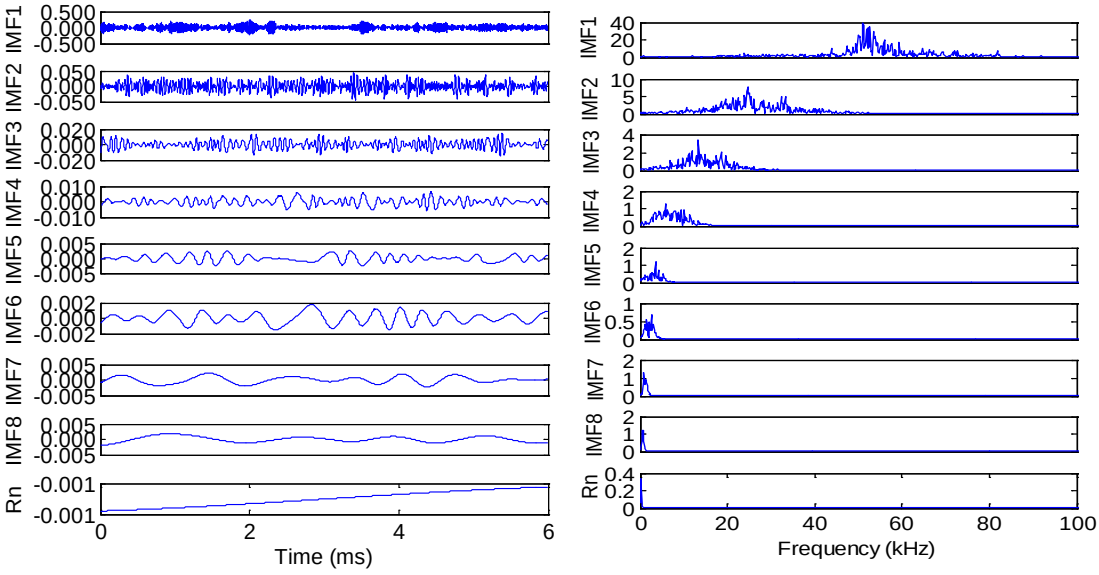

Fig. 15. EMD results of the signal from sensor 3.

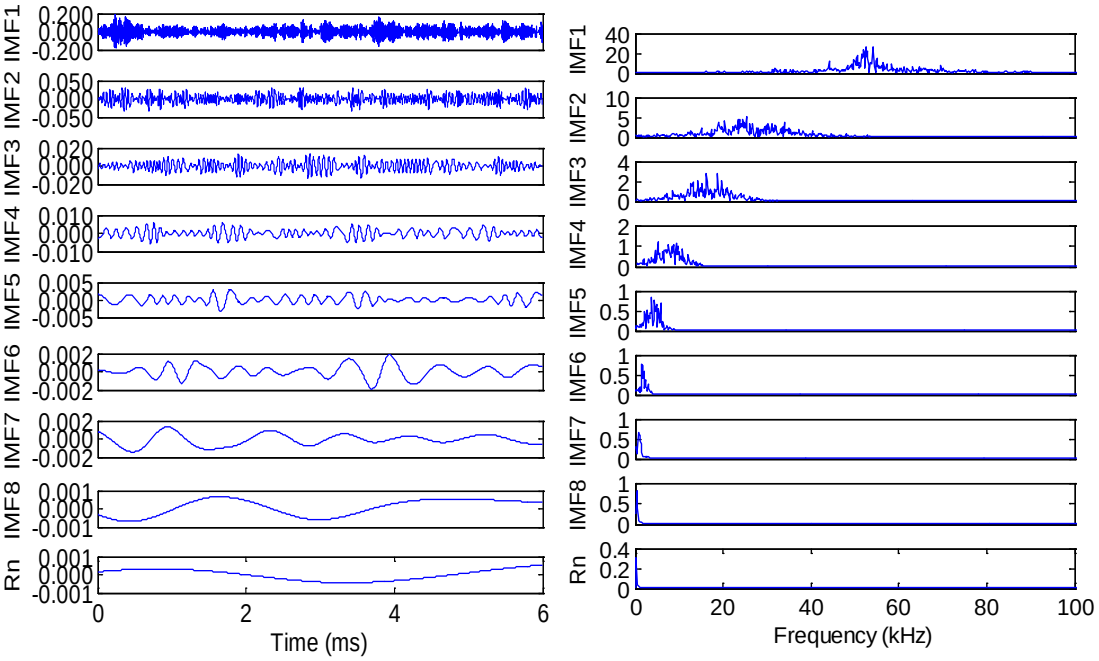

Fig. 16. EMD results of the signal from sensor 4.

It can be seen from Fig. 13-16 that eight IMF components together with a residual R_n have been generated for each AE signal received. In the time domain (plots on the left-hand-side of Fig. 13-16), the amplitudes of all the IMF components decrease by several orders of magnitudes from the highest value in IMF1 to the lowest in IMF8. In the frequency domain, the same trend is observed, i.e. IMF1 has the highest instantaneous frequency and IMF8 has the lowest instantaneous frequency. Therefore,

IMF components that contain low values of the signal magnitude and frequency can be safely ignored. Such components are more likely produced from various noise sources as indicated in Fig. 9.

Furthermore, the energy ratio of each IMF component can be calculated as follows:

$$E_{IMF\,i} = \frac{1}{N}\sum_{m=0}^{N-1} h_i(m)^2 \tag{8}$$

$$R_{IMF\,i} = \frac{E_i}{\sum_{i=1}^{8} E_i} \times 100\% \tag{9}$$

where $h_i(m)$ stands for the i^{th} IMF, N is the length of the signal, $E_{IMF\,i}$ and $R_{IMF\,i}$ represent the energy of the i^{th} IMF and its energy ratio. The results are summarized in Table 2. It can be seen that IMF1 and IMF2 contain over 98% of the energy in each signal and hence reflect the main information of the signal.

Table 2
Energy ratio of each IMF component (%).

	$R_{IMF\,1}$	$R_{IMF\,2}$	$R_{IMF\,3}$	$R_{IMF\,4}$	$R_{IMF\,5}$	$R_{IMF\,6}$	$R_{IMF\,7}$	$P_{IMF\,8}$
Sensor 1	92.46	6.37	0.91	0.17	0.04	0.02	0.02	0.01
Sensor 2	94.53	4.81	0.48	0.09	0.04	0.02	0.01	0.01
Sensor 3	94.72	4.50	0.59	0.11	0.03	0.03	0.01	0.01
Sensor 4	93.19	5.59	0.92	0.20	0.05	0.02	0.02	0.01

Therefore, a new signal is reconstructed using IMF1 and IMF2 only to represent the original signal, and the low energy components can be safely ignored:

$$S_{new}=IMF1+IMF2 \tag{10}$$

Fig. 17 shows the waveforms of the reconstructed signals.

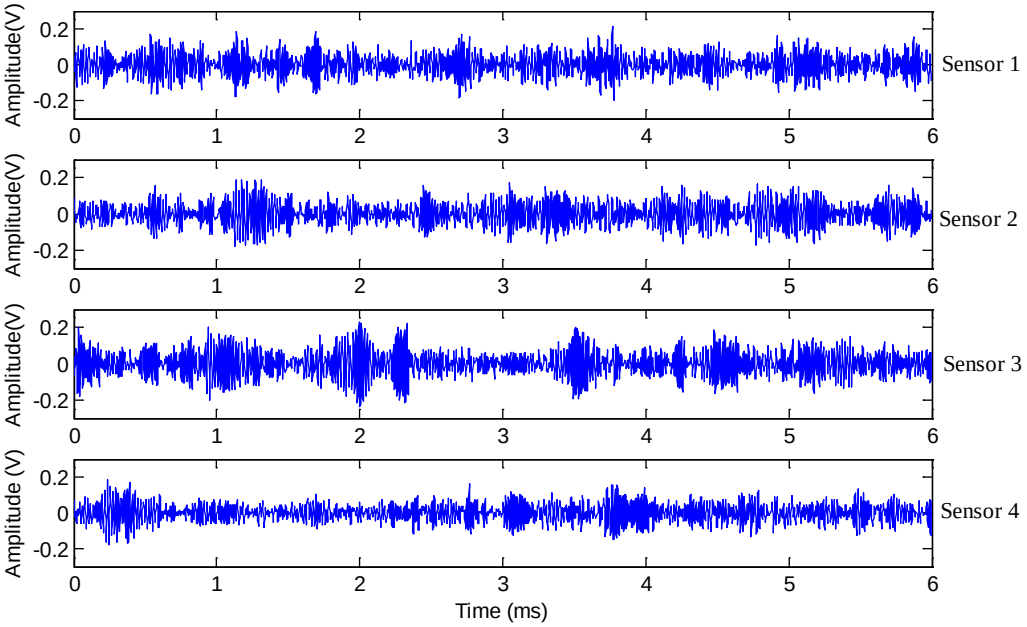

Fig. 17. Reconstructed waveforms for the AE signals.

4.4. Leak localization and error analysis

Fig. 18 shows the correlation functions between the reconstructed signals from sensor 1 and sensors 2-4 and the resulting correlation coefficients are 0.71, 0.50 and 0.48, respectively. It is suggested that sensors 1 and 2 show the strongest correlation while sensors 1 and 4 show the weakest correlation.

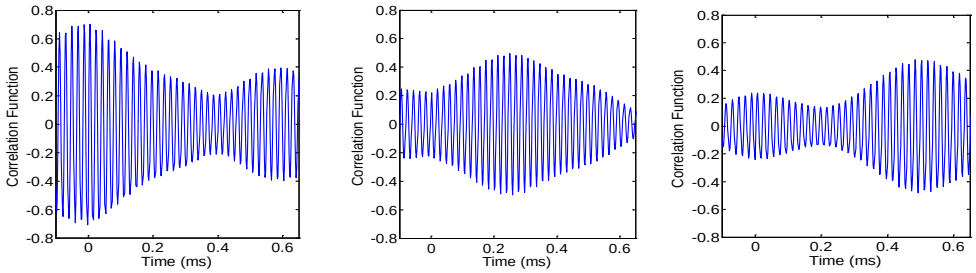

(a) Sensors 1 and 2 (b) Sensors 1 and 3 (c) Sensors 1 and 4

Fig. 18. Correlation functions between signals from sensor 1 and other sensors.

The location of the dominant peak on the time axis in the correlation function represents the time difference (Δt) between the two signals. Δt is used to calculate the location of the leak source using equation (5), together with the speeds of the AE wave obtained from the Nielsen-Hsu Pencil Lead Break Tests (Section 4.1). Table 3 lists the distance difference, Δd, and the localization errors using different pairs of sensors.

Table 3

Localization errors using different pairs of the sensors.

Sensor Pair	Correlation Coefficient	Acoustic Wave Speed (m/s)	*Time difference (ms)*	*Distance difference (m)*	*Error* (m)	Sensors Spacing (m)	Relative Error (%)
1 and 2	0.71	Longitudinal (5070)	0.002	0.01	0.01	2	0.5
		Transverse (3268)		0.01	0.01		0.5
1 and 3	0.50	Longitudinal (5070)	0.26	1.32	0.32	3	10.7
		Transverse (3268)		0.85	0.15		5
1 and 4	0.48	Longitudinal (5070)	0.49	2.48	0.48	4	12
		Transverse (3268)		1.60	0.40		10

It can be seen from Table 3 that the localization error using sensors 1 and 2 is much smaller than the other two pairs. This is because sensors 1 and 2 are symmetrical about the leak hole. Therefore the two AE signals have the same degree of attenuation and dispersion which makes them have the strongest correlation. This result reflects, to some extent, the influence of the signal attenuation and dispersion along the pipeline on the quality of the signals. With increasing asymmetry of the sensors with reference to the leak source, the correlations between the signals become weak and the localization errors increase.

Table 3 also shows that, in the case of sensors 1 and 2, the localization error is same when the transverse wave speed and longitudinal wave speed are used. However, with increasing asymmetry of the sensors' locations with reference to the leak source, i.e. sensors 1 and 3, sensors 1 and 4, the localization error is smaller when the transverse wave speed is used instead of the longitudinal wave speed. The reasons for this is that the longitudinal wave usually has the lower amplitude than the transverse wave, so it only accounts for a smaller proportion in the AE signal although its speed is higher, as seen in Fig. 9. In addition, the longitudinal wave can propagate in solid, liquid and air while the transverse wave can only propagate in the solid pipeline wall. Therefore the longitudinal wave has more energy attenuation than the transverse wave.

The results in Table 3 show a good consistency between the correlation coefficient and the accuracy of the localization, i.e. the bigger of the correlation coefficient between a pair of signals, the more accurate of the leak location result. Since the sensor array will be installed in the industrial processes, a data fusion method based on correlation coefficient of the signals should be a reasonable and effective approach to accurately localize the leak source. The weight coefficient u_i and localization error ε_i can be

calculated using equations (11) and (12), respectively, as follows:

$$\varepsilon = \sum_{i=1}^{3} u_i \varepsilon_i \tag{11}$$

$$u_i = \frac{r_i}{\sum_{i=1}^{3} r_i} \tag{12}$$

where r_i and ε_i represent the correlation coefficient and the error used the i^{th} pair of the AE sensors, respectively.

This data fusion method fully considers the reliability of measurement results from multi sensors. The localization error is 4.5% when the transverse wave speed is used and 6.8% when the longitudinal wave speed is used. The results show that the technique has a good performance in the leak localization.

5. Conclusions

In this paper investigations have been carried out experimentally on the potential use of low frequency and narrow band AE sensors for the localization of accidental CO_2 leak from long distance transportation pipelines. The influences of signal attenuation and dispersion have been effectively minimized using the empirical mode decomposition technology which has shown a good performance in processing the non-linear and non-stationary AE signals. Newly reconstructed AE signals, based on the main energy components of the IMF, i.e. IMF1 and IMF2 (up to 98%), have been employed to predict the location of the leak through cross-correlation of the reconstructed signals. There is a good consistency between the correlation coefficient and the accuracy of the leak localization. When the two AE sensors are symmetrically installed about the leak source, the maximal correlation coefficient has been obtained and the localization error is less than 1%. With an increasing asymmetry of the sensor installations with respect to the source of the leak, the correlation between the signals becomes weak and the localization error increases. Furthermore, the speeds of the transverse and the longitudinal waves are measured using the Nielsen-Hsu Pencil Lead Break Test. These speeds have been used to determine the location of the leak. It is observed that the localization errors are smaller when the transverse wave speed is used. Finally, a data fusion method based on the correlation coefficient has been employed. The results have demonstrated that the system gives a localization error of 4.5%. In summary, low frequency and narrow band AE sensors together with empirical mode

decomposition and signal reconstruction have a good potential to localize leaks from a long distance CO_2 pipeline.

Acknowledgement

The authors wish to acknowledge the Chinese Ministry of Science and Technology (MOST) and the Chinese Ministry of Education for providing financial support for this research as part of the 111 Talent Introduction Projects (B13009) at North China Electric Power University. This work was also supported by the Fundamental Research Funds for the Central Universities (No. 2014XS40). Xiwang Cui would like to thank the China Scholarship Council for offering an academic exchange grant for his visit to the University of Kent.

References

[1] S. M. Benson, T. Surles. Carbon dioxide capture and storage: An Overview with emphasis on capture and storage in deep geological formations, Proceedings of the IEEE, 2006, 94(10), pp.1795-1805.

[2] J. Gale, J. Davison. Transmission of CO_2 safety and economic considerations. Energy, 2004, 29(10), pp.1319-1328.

[3] G. J. Zhang, Y. P. Li, Q. B. Li. A miniaturized carbon dioxide gas sensor based on infrared absorption. Optics and Lasers in Engineering, 2010, 48(12), pp.1206-1212.

[4] A. Somov, A. Baranov, D. Spirjakin, A. Spirjakin, V. Sleptsov, R. Passerone. Deployment and evaluation of a wireless sensor network for methane leak detection. Sensors and Actuators A: Physical, 2013, 202, pp.217–225.

[5] S. Huang, W. Lin, M. Tsai, M. Chen. Fiber optic in-line distributed sensor for detection and localization of the pipeline leaks. Sensors and Actuators A: Physical, 2007, 135(2), pp.570-579.

[6] Z. Guan, M. Lewander, R. Gronlund, H. Lundlerg, S. Svanberg. Gas analysis within remote porous targets using LIDAR multi-scatter techniques. Applied Physics B: Lasers and Optics, 2008, 93(2), pp.657-663.

[7] I. M. Perez de Vargas-Sansalvador, C. Fay, T. Phelan, M. D. Femandez-Ramos, L. F. Capitan-Vallvey, D. Diamond, F. Benito-Lopez. A new light emitting diode-light emitting diode portable carbon dioxide gas sensor based on interchangeable membrane system for industrial applications. Analytica Chimica Acta, 2011, 699(2), pp. 216-222.

[8] J. A. Hogan, J. A. Shaw, R. L. Lawrence, J. L. Lewicki, L. M. Dobeck, L. H. Spangler. Detection of leaking CO_2 gas with vegetation reflectances measured by a low-cost multispectral imager. IEEE Journal of Selected Topics in Applied Earth Observations and Remote Sensing, 2012, 5(3), pp. 699-706.

[9] P. Murvay, I. Silea. A survey on gas leak detection and localization techniques. Journal of Loss Prevention in the Process Industries, 2012, 25(6), pp. 966-973.

[10] G. Zhang, Y. Li, Q. Li. A miniaturized carbon dioxide gas sensor based on infrared absorption. Optics and Lasers in Engineering, 2010, 48(12), pp. 1206-1212.

[11] V. L. Kasyutich, P. A. Martin. A CO_2 sensor based upon a continuous-wave thermoelectrically-cooled quantum cascade laser. Sensors and Actuators B: Chemical, 2011, 157, pp. 635-640.

[12] V. R. Lakkaraju, X. Zhou, M. E. Apple, A. Cunningham, L. M. Dobeck, K. Gullickson, L. H. Spangler. Studying the vegetation response to simulated leakage of sequestered CO_2 using spectral vegetation indices. Ecological Informatics, 2010, 5(5), pp.379–389

[13] S. J. Martin, G. C. Frye, J. J. Spates, M. A. Butler. Gas sensing with acoustic devices. IEEE Ultrasonics Symposium Proceedings, 1996, 1, pp. 423-434.

[14] R. K. Miller, A. A. Pollock, D. J. Watts, J. M. Carlyle, A. N. Tafuri, J. J. Yezzi. A reference standard for the development of acoustic emission pipeline leak detection techniques. Non-Destructive Testing and Evaluation (NDT & E) International Journal, 1999, 32(1), pp. 1-8.

[15] K. Adefila, Y. Yan. A compendium of CO_2 leakage detection and monitoring techniques in carbon capture and storage (CCS) pipelines. EUROCON, 2013 IEEE, pp. 1328-1335.

[16] A. Mostafapour, S. Davoudi. Analysis of leakage in high pressure pipe using acoustic emission method. Applied Acoustics, 2013, 74, pp.335-342.

[17] [On-line] Soundwel Technology, Acoustic emission technology application, http://wenku.baidu.com/link?url=fDIrbgs2br4T4yOpuUPUjOCfruLJjtMiBysC21TbD9a_1vkZGR2M5iDYHBrsJo-WmoZKl84idYjKiiBbStKiRqQSmLfAMtqjUC82G3xLAmW. Accessed 2015/3/24.

[18] W. H. Prosser, K. E. Jackson, S. Kellas, B. T. Smith, J. Mckeon, A. Friedman. Advanced waveform-based acoustic emission detection of matrix cracking in composites. Materials Evaluation, 1995, 9, pp. 1052-1058.

[19] P. Wilcox, M. Lowe, P. Cawley. The effect of dispersion on long-range inspection

using ultrasonic guided waves. Non-Destructive Testing and Evaluation (NDT & E) International Journal, 2001, 34, pp. 1-9.

[20] B. Liu, S. Riemenschneider, Y. Xu. Gearbox fault diagnosis using empirical mode decomposition and Hilbert spectrum. Mechanical Systems and Signal Processing.2006, 20(3), pp. 718-734.

[21] Z. Shen, N. Feng, Y. Shen, C. Lee. A ridge ensemble empirical mode decomposition approach to clutter rejection for ultrasound color flow imaging. IEEE Transactions on Biomedical Engineering, 2013, 60(6), pp. 1477-1487.

[22] D. Huang, J. Zhao, J. Sun. Practical implementation of Hilbert-Huang transform algorithm. Acta Oceanologica Sinica, 2003, 22(1), pp. 1-14.

[23] Y. A. Khulief, A. Khalifa, R. B. Mansour, M. A. Habib. Acoustic detection of leaks in water pipelines using measurements inside pipe. Journal of Pipeline Systems Engineering and Practice, 2011, 3(2), pp. 47-54.

[24] S. Li, Y. Wen, P. Li, J. Yang, L. Yang. Determination of acoustic speed for improving leak detection and location in gas pipelines. Review of Scientific Instruments, 2014, 85(2), pp. 024901-11.

[25] X. Qian, Y. Yan. Flow measurement of biomass and blended biomass fuels in pneumatic conveying pipelines using electrostatic sensor-arrays. IEEE Transactions on Instrumentation and Measurement, 2012, 61(5), pp. 1343–1352.